6th International Conference on Structural Engineering and Construction Management 2015,
Kandy, Sri Lanka, 11th-13th December 2015

SECM/15/170

Fatigue Life Prediction of Steel Bridges with High Amplitude Loadings

P.A.K. Karunananda[1], T.M. pallewatta[1], P.B.R. Dissanayake[2], M. Ohga[3] and S.A.S.C.Siriwardane[4]

[1]Department of Civil Engineering, The Open University of Sri Lanka, Sri Lanka
[2]Department of Civil Engineering, University of Peradeniya, Sri Lanka
[3]Department of Civil and Environmental Engineering, Ehime University, Japan
[4]Department of Mechanical Engineering, University of Stavanger, Norway

Abstract: This paper presents a new fatigue model to predict life of steel bridges considering the effect of high amplitude loading. It consists of a modified strain-life curve and a new strain based damage index. Modified strainlife curve consists of Coffin-Manson relation in low cycle fatigue region and a new strain-life curve in high cycle fatigue region. The damage variable is based on a modified von Mises equivalent strain to account for the effects of loading non-proportionality and strain path orientation in multiaxial stress state. The proposed model was verified with experimental test results of two materials available on the literature. Then, it was illustrated with an old riveted wrought iron railway bridge. The obtained results verify the effectiveness of the proposed model over commonly used Miner's rule based life prediction of steel bridges.

Keywords: High cycle fatigue, low cycle fatigue, steel bridges, life prediction, high amplitude loading.

1. Introduction

Bridges are generally subjected to low amplitude loading by usual traffic. As a result, bridge members generally experience high cycle fatigue (HCF) damage. During their service life, bridges may also be subjected to high amplitude loading due to earthquakes, unexpected stress concentrations and etc. When a bridge is subjected to high amplitude loading, some members may undergo inelastic stresses. These inelastic stresses may cause low cycle fatigue (LCF) damage during the high amplitude loading while subjecting to HCF in service conditions. This combined damage of HCF and LCF may cause a reduced life of members (Kondo and Okuya 2007). In addition, bridges connections are generally subjected to multiaxial stress states and combined with HCF and LCF create a complexity in accurate estimation of fatigue life.

Most of existing fatigue life research of bridges is based on multiaxial high cycle fatigue. To the knowledge of authors, there is almost no literature regarding high amplitude loading effects on bridges. However, in other fields such as aircraft and automobile engineering, von Mises equivalent strain and Coffin-Manson strain-life curve are used with Miner's rule as the general method to estimate the life due to high and low amplitude loadings (Suresh 1998). The Miner's rule is the simplest and the most widely used fatigue life prediction technique. One of its interesting features is that life calculation is simple and reliable when the detailed loading history is unknown. However under many variable amplitude loading conditions, Miner's rule based life predictions have been found to be unreliable since it cannot capture loading sequence effect (Siriwardane et al. 2008). In addition, von Mises equivalent strain cannot capture the effects due to non-proportional loading and orientation of strain path (Borodii and Adamchuk 2009). As a result, it usually predicts inaccurate fatigue life.

These reasons raise the question about accuracy of the Miner's rule based life estimation for high and low amplitude loadings. Therefore, it is necessary to have a comprehensive model, which is based on commonly available material properties, to estimate more accurately the life due to high and low amplitude loadings. The objective of this paper is to propose a new model to accurately estimate the fatigue life (crack initiation life) when a bridge is subjected to high amplitude loading in addition to the usual low amplitude loading.

2. Proposed Fatigue Model

This section proposes the new fatigue model to consider the effect of high amplitude loading.

Initially, the details relevant to proposed damage variable, modified strain-life fatigue curve are discussed. Then, it is followed by the proposed damage indicator.

2.1 Damage variable

The proposed damage variable for multiaxial stress state is given as,

$$\varepsilon_{eq} = (1+\alpha\phi)(1+kSin\varphi)\varepsilon_{VM} \quad (1)$$

where ε_{eq} is the equivalent strain amplitude in the multiaxial stress state, α is the material parameter for loading non-proportionality, ϕ is the cycle non-proportionality parameter, k is the material parameter for strain path orientation, φ is the angle between principal direction and applied strain path and ε_{VM} is the von Mises equivalent strain as given

$$\varepsilon_{VM} = \frac{1}{(\sqrt{2}\times(1+\nu))}\left[\begin{array}{l}(\varepsilon_{xx}-\varepsilon_{yy})^2+(\varepsilon_{yy}-\varepsilon_{zz})^2 \\ +(\varepsilon_{zz}-\varepsilon_{xx})^2 \\ +\frac{3}{2}\times(\gamma_{xy}^2+\gamma_{yz}^2+\gamma_{zx}^2)\end{array}\right]^{1/2} \quad (2)$$

where ν is the Poison ratio, ε and γ are the axial and shear strain amplitudes in respective planes.

The first expression in parentheses of equation (1) is the degree of additional strain hardening depending on the cycle geometry to account for non-proportional loading. The second expression in parentheses is strain hardening depending on the orientation of the cyclic strain path for proportional loading. The material parameters (α and k) have to be estimated by additional testing of the material. ϕ and φ can be estimated for given strain path considering cycle geometry and its orientation, respectively (Borodii and Adamchuk 2009).

2.2 Strain-life curve

To take account the damage dependent effect in high and low amplitude loading, it is necessary to modify the strain-life fatigue curve in HCF regime. The proposed curve consists of two parts as shown in Figure 1. The first part of the curve describes fatigue life of plastic strain $(\varepsilon_{eq} \geq \varepsilon_y)$ cycles which usually affects LCF. To describe this part, Coffin-Manson strain-life curve is utilized as shown below.

$$\varepsilon_{eq} = \frac{\sigma_f^{'}}{E}(2N)^b + \varepsilon_f^{'}(2N)^c \quad (3)$$

where ε_{eq} is the equivalent strain amplitude in multiaxial stress state, N is the number of cycles to failure, $\sigma_f^{'}$ is the fatigue strength coefficient, b is the fatigue strength exponent, $\varepsilon_f^{'}$ is the fatigue ductility coefficient, c is the fatigue ductility exponent and E is the elastic modulus of the material.

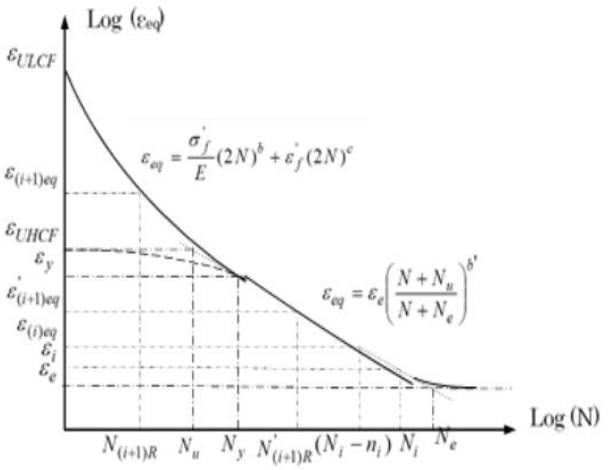

Figure 1: Schematic representation of the proposed strain-life curve

The ultimate strain of low cycle fatigue, $(\varepsilon)_{ULCF}$ which is the strain amplitude corresponding to failure in half reversal (a quarter of a cycle) is obtained from equation (3) as,

$$(\varepsilon)_{ULCF} = \varepsilon_f^{'} \quad (4)$$

The second part of the curve describes the fatigue life of elastic strain cycles which usually $(\varepsilon_{eq} < \varepsilon_y)$ affects HCF. This part of curve represents hypothetical fully known curve. The shape of the curve is obtained by directly transforming the previous fully known stress-life curve (Siriwardane et al. 2008) to elastic strain-life curve as shown below.

$$\varepsilon_{eq} = \varepsilon_e\left(\frac{N+N_u}{N+N_e}\right)^{b'} \quad (5)$$

where ε_e is the strain amplitude of the fatigue limit, N_e is the number of cycles to failure at strains of ε_e. The ε_y and N_y are the yield strain

and the corresponding number of cycles to failure. The $b^{'}$ is the slope of the finite life region of the curve. The $(\varepsilon)_{UHCF}$ is the ultimate strain of HCF which is the elastic strain amplitude corresponding to half reversal (a quarter of a cycle) is expressed as,

$$(\varepsilon)_{UHCF} = \left(\frac{\sigma_u}{E}\right) \tag{6}$$

where σ_u is the ultimate tensile strength of the material. The N_u is the number cycles corresponding to the intersection of the tangent line of the finite life region and the horizontal asymptote of the ultimate elastic strain amplitude $(\varepsilon)_{UHCF}$ as shown in Figure 1.

2.3 Damage indicator

The proposed damage indicator considers combined damage of high and low amplitude loadings. The hypothesis behind this fatigue law is that if the physical state of damage is the same, then fatigue life depends only on the loading condition. Suppose a component is subjected to a certain equivalent strain amplitude $(\varepsilon)_i$ of n_i number of cycles at load level *i*. N_i is the fatigue life (number of cycles to failure) corresponding to $(\varepsilon)_i$ (Figure 1). Therefore, the reduced life at the load level *i* is obtained as (N_i–n_i). $(\varepsilon)_{(i)eq}$ The damage equivalent strain (Figure 1), corresponding to the failure life (Ni–ni) is defined as ith level damage equivalent strain. Then, the new damage indicator, Di is stated as,

$$D_i = \frac{(\varepsilon)_{(i)eq} - (\varepsilon)_i}{(\varepsilon)_u - (\varepsilon)_i} \tag{7}$$

where the $(\varepsilon)_u$ is

$$(\varepsilon)_u = \begin{cases} \varepsilon_{ULCF} & (\varepsilon)_i \geq \varepsilon_y \\ \varepsilon_{UHCF} & (\varepsilon)_i < \varepsilon_y \end{cases} \tag{8}$$

At the end of i^{th} loading level, damage D_i has been accumulated (occurred) due to the effect of $(\varepsilon)_{i+1}$ loading cycles, the damage is transformed to load level *i+1* as below.

$$D_i = \frac{(\varepsilon)^{'}_{(i+1)eq} - (\varepsilon)_{i+1}}{(\varepsilon)_u - (\varepsilon)_{i+1}} \tag{9}$$

and $(\varepsilon)_u$ is expressed

$$(\varepsilon)_u = \begin{cases} \varepsilon_{ULCF} & (\varepsilon)_{i+1} \geq \varepsilon_y \\ \varepsilon_{UHCF} & (\varepsilon)_{i+1} < \varepsilon_y \end{cases} \tag{10}$$

Then, $(\varepsilon)^{'}_{(i+1)eq}$ is the damage equivalent strain at loading level *i+1* and it is calculated as,

$$(\varepsilon)'_{(i+1)eq} = D_i[(\varepsilon)_u - (\varepsilon)_{i+1}] + (\varepsilon)_{i+1} \tag{11}$$

The corresponding equivalent number of cycles to failure $N'_{(i+1)R}$ is obtained from the strain-life curve as shown in Figure 1. The $(\varepsilon)_{i+1}$ is the equivalent strain at the level i+1 and supposing that it is subjected to number of cycles, then the corresponding residual life at load level i+1, $N_{(i+1)R}$ is calculated as,

$$N_{(i+1)R} = N'_{(i+1)R} - n_{(i+1)} \tag{12}$$

Therefore, strain $(\varepsilon)_{(i+1)eq}$, which corresponds to $N_{(i+1)R}$ at load level *i+1,* is obtained from the strain-life curve as shown in Figure 1. Then the cumulative damage at the end of load level *i+1* is defined as,

$$D_{(i+1)} = \frac{(\varepsilon)_{(i+1)eq} - (\varepsilon)_{i+1}}{(\varepsilon)_u - (\varepsilon)_{i+1}} \tag{13}$$

This is carried out until D_i is equal to 1.

3. Experimental verification of The Proposed model

This section explains the verification of the proposed fatigue model. Experimental test results of two materials were used for this purpose: S304L stainless steel and Haynes 188.

3.1 Verification for S304L Steel

Random variable fatigue test performed by Colin and Fatami 2010 were used to verify the proposed fatigue model. Experimental results were compared with the predicted lives of the proposed fatigue model as well as the Miner's rule based previous model. The obtained comparisons are given in Table 1.

Table 1: Experimental summary and predicted fatigue lives of S304L steel

Test	Maximum strain	Minimum strain	Experimental life (blocks)		Predicted life (blocks)	
			Test life	Average life	Previous model	Proposed model
1	0.001	-0.001	211			
2	0.001	-0.001	196			
				203	259	239
3	0.005	-0.005	1601			
4	0.005	-0.005	1740			
				1671	2789	2118
5	0.003	-0.003	14463			
6	0.003	-0.003	15666			
				15065	20122	10075

In above table, first two tests are in LCF region while other four are combined HCF and LCF tests. If the percentage variations of the predictions are estimated with the experimental results, Miner's rule gives a percentage variation of 26.59% while the proposed model gives 15.39%. Therefore, Proposed model based fatigue lives are more accurate than previous model predictions.

3.2 Verification for Haynes 188

Block loading fatigue tests performed by Bonacuse and Kalluri 2002 were used to verify the proposed fatigue model. Here, axial (A) and torsional (T) block loading tests were performed in four different sequences (AA, TT, AT and TA) as shown Table 4. The first loading block is in the high cycle fatigue region and the second is in the low cycle fatigue region. The material parameter, *k*, was estimated as 0.17 by constant amplitude testing given in Kalluri and Bonacuse 1999. Experimental results were compared with the predicted lives of the proposed fatigue model as well as previous model as given in Table 1.

Table 2: Experimental summary and predicted fatigue lives of Haynes 188

	First load level		Second load level			Predicted life (cycles)	
Test	Strain amplitude	No of cycles (n_1)	Strain amplitude	No of cycles (n_2)	Experimental life (n_1+n_2)	Previous model	Proposed model
AA1	0.0067	3926	0.0203	789	4715	4365	4413
AA2	0.0066	7851	0.0202	758	8509	8249	8337
AA3	0.0066	15702	0.0203	659	16361	15977	16147
AA4	0.0066	23553	0.0205	815	24368	23709	23931
TT1	0.0120	5857	0.0345	1250	7107	7276	7414
TT2	0.0120	11714	0.0349	1100	12814	12923	13189
TT3	0.0121	23427	0.0347	1343	24770	24316	24832
TT4	0.0119	35141	0.0347	1467	36608	35677	36219
TT5	0.0120	40998	0.0349	1294	42292	41348	41812
AT1	0.0069	3926	0.0348	1189	5115	5084	5345
AT2	0.0069	7851	0.0347	1218	9069	8660	9093
AT3	0.0065	15702	0.0344	930	16632	16058	16600
AT4	0.0066	23553	0.0346	1253	24806	23885	24185
TA1	0.0121	5857	0.0201	560	6417	6316	6367
TA2	0.0120	11714	0.0203	494	12208	12133	12216
TA3	0.0119	23427	0.0200	459	23886	23740	23907
TA4	0.0119	35141	0.0204	427	35568	35322	35588

The percentage variations of predicted lives from experimental lives for previous and proposed models were estimated as 0.74% and 0.62%, respectively. Therefore, the predicted fatigue lives by the proposed fatigue model are more accurate than previous model predictions.

3.3 Case study

This section explains the application of the proposed model to a riveted wrought iron railway bridge. The selected bridge is one of the longest railway bridges in Sri Lanka and a view of the bridge is shown in Figure 2 (a). The evaluations are especially based on secondary stresses and strains, which are generated around the riveted connection of the member due to stress concentration effect of primary stresses caused by usual traffic (low amplitude) and earthquake (high amplitude) loadings. The selected member is shown in Figure 2 (b).

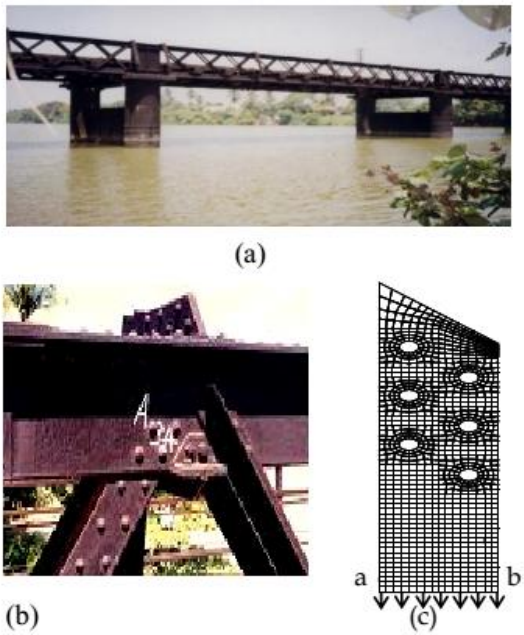

Figure 2: Views of (a) the bridge; (b) considered member and (c) the FEM mesh.

The fatigue life is estimated based on the state of strain considering all rivets are in active state while they have no clamping force. The clamping force is generally defined as the compressive force in plates which is induced by the residual tensile force in the rivet. Since there are no clamping force (value of clamping force is zero), connected members are considered to subject to the biaxial stress state. Then, a critical member without rivets can be considered to analyze the biaxial state of stress of a 2D finite element analysis. The nine node isoperimetric shell elements were used for the FE analysis as shown in Figure 2(c). Earthquake (high amplitude loading) was considered to occur at different times in bridge life (10, 50, 75 and 100 years) as given in Table 3.

Table 3: Fatigue life of the member for different earthquake occurrences

Time of earthquake (after construction, years)	Previous model (Miner's rule)		Proposed model	
	Fatigue life (years)	Percentage reduction of life (%)	Fatigue life (years)	Percentage reduction of life (%)
10	127.7	5.0	130.9	19.6
50	127.7	5.0	109.6	32.7
75	127.7	5.0	116.3	28.6
100	127.7	5.0	130.5	19.9
No earthquake	134.5	-	162.8	-

It is assumed that usual traffic load is followed after the earthquake. The fatigue life of the member was estimated using two approaches: (1) proposed model; (2) previous model (Coffin-Manson curve with the Miner's rule) and the obtained results are given in Table 3. The results indicate fatigue damage caused by earthquake loading causes an appreciable reduction of bridge life. There, the percentage reduction of life is the highest when the earthquake occurs 50 years after the construction. If the earthquake magnitude is increased, the highest percentage reduction of life occurs earlier than 50 years. Therefore, the magnitude of the earthquake load has an effect in estimating the year with the highest percentage reduction. For the previous model, the reduction of service life is constant (5%) irrespective of time of earthquake occurrence since Miner's rule cannot represent the loading sequence effect. These results show the effectiveness of the proposed method over previous model in life prediction.

The differences of case study results confirm the importance of considering high amplitude loading to estimate the fatigue life of existing steel bridges in addition to usual traffic loadings.

5. Conclusions

A new model for life estimation of high amplitude loading was proposed. Verification of the model was conducted by comparing the predicted lives with experimental lives of two materials. It was shown that the proposed fatigue model can represent the effect of high amplitude loading better than the previous model where detailed stress histories are known. The proposed fatigue model was utilized to estimate the fatigue life of a bridge member. Case study realized the importance of consideration of the high amplitude loading caused by earthquake in addition to low amplitude loading due to usual traffic loading in steel bridges. The effectiveness of the proposed model over the Miner's rule based previous model was verified.

References

[1] Bonacuse P and Kalluri S (2002). Sequenced axial and torsional cumulative fatigue: low amplitude followed by high amplitude loading, Biaxial/Multiaxial Fatigue and Fracture, Elsevier.

[2] Borodii MV and Adamchuk MP (2009). Life assessment for metallic materials with the use of the strain criterion for low cycle fatigue. International Journal of Fatigue. 31, pp. 1579-1587.
[3] Colin L and Fatami A (2010). Variable amplitude cyclic deformation and fatigue behavior of stainless steel 304L including step, periodic and random loading. Fatigue and Fracture of Engineering Materials and Structures. 33, pp. 205-220.
[4] Kalluri S and Bonacuse PJ (1999). Cumulative axial and torsional fatigue: an investigation of load-type sequencing effects. ASTM symposium on multiaxial fatigue and deformation: testing and production, Seattle, WA
[5] Kondo Y and Okuya K (2007). The effect of seismic loading on the fatigue strength of welded joints. Material Science and Engineering A. 468-470. pp. 223-229.
[6] Siriwardane S, Ohga M, Dissanayake R and Taniwaki K (2008). Application of new damage indicator-based sequential law for remaining fatigue life estimation of railway bridges. Journal of Constructional Steel Research. 64(2). pp. 228-237.
[7] Suresh S (1998). Fatigue of Materials, UK: Cambridge University Press, Cambridge.